THESIS

DIURNAL AND SEASONAL PREDICTABILITY OF ENVELOPE PRESSURES DRIVING NATURAL INFILTRATION IN RESIDENTIAL BUILDINGS

Submitted by

Dominic Bledsoe

Department of Mechanical Engineering

In partial fulfillment of the requirements

For the Degree of Master of Science

Colorado State University

Fort Collins, Colorado

Fall 2024

Master's Committee:

Advisor: Tami Bond

Christian L'Orange
Delphine Farmer

ABSTRACT

DIURNAL AND SEASONAL PREDICTABILITY OF ENVELOPE PRESSURES DRIVING NATURAL INFILTRATION IN RESIDENTIAL BUILDINGS

This study examines the dynamics of residential building envelope pressures by predicting and comparing time series site-specific weather conditions at minute-level resolution. Utilizing theoretically established relationships of both stack and wind effects, this research examines the predictability and accuracy of envelope pressures under different weather conditions. When high wind effects are removed, the Mean Absolute Error (MAE) in stack pressure predictions are minimized, typically falling below 0.24 Pa. The use of airport weather data, even after correcting for height difference and terrain, was found to be inconducive to prediction, highlighting the preference for site-specific measurements to enhance prediction accuracy. This research utilizes minute-level data for real-time environmental monitoring, aiming to inform pressurization or integrate predictive models for dynamic indoor air quality management. The findings contribute to the field by offering a practical approach to measuring and predicting residential air exchange rates, providing insights that could lead to improved health outcomes and energy efficiency in homes.

TABLE OF CONTENTS

LIST OF TABLES

LIST OF FIGURES

INTRODUCTION AND BACKGROUND

Residential environments are a key space for understanding the impacts of indoor air quality and occupants' well-being because people spend 70% of their lives in their homes [1]. Therefore, health stressors present in these spaces become significant exposure risks, especially for sensitive groups. Understanding how airflow throughout the home changes with time could enable better air transport management to carry outdoor pollutants inside or replace indoor pollutants with fresh air, minimizing exposure to health stressors.

A key metric of residential airflow is Air Exchange Rate. This value, usually expressed as air changes per hour (ACH) refers to the number of times the air volume in a space is completely removed and replaced in an hour. Air exchange includes infiltration, airflow from outdoors in, and exfiltration, the airflow from indoors out. In the absence of mechanical ventilation, infiltration balances exfiltration, and the term “infiltration” will be used throughout this document to signify both. The rate of air exchange of a structure under naturally ventilated conditions is:

$$ACH = \frac{Q_{inf}}{V} = \frac{Q_{exf}}{V} \tag{1}$$

where V is the volume of the building.

ACH values for residential buildings vary widely based on construction practices and climate, with changes to building codes and construction practices over time reducing leakage rate. A typical range for homes that have a high rate of natural leakage is 1 to 1.5 ACH, while tighter homes range from 0.2 to 0.5 ACH [2]. Persily et al. demonstrated that across various U.S. climates, homes built after 1970 had significantly lower ACH than those built before that time [3]. Air exchange is also affected by occupancy patterns and ventilation strategies.

A home's ACH is directly related to the concentration and migration of pollutants. Tighter homes reduce energy consumption for space conditioning, but low ACH values may result in pollutants generated indoors such as VOCs from cooking being trapped within the home. Modern building codes and standards such as ASHRAE Standard 62.2, now mandate that new construction implement mechanical ventilation systems to ensure adequate ventilation in increasingly airtight homes [4]. However, pollutant concentrations are also affected by the outdoor environment, and this influence occurs more quickly in homes with high ACH values.

Theory of Residential Building Leakage

Theoretical predictions of airflow Q through an individual crack j can be described as:

$$Q_j = K_j(\Delta P_j)^n \quad (2)$$

where ΔP_j is the pressure difference across the crack, K_j is a coefficient that includes the crack area and any discharge coefficient, and n is an exponent that encapsulates the type of flow through the crack (0.5 for turbulent, 1 for laminar).

A blower door test is a common technique for estimating total leakage [5]. In this method, a large panel is installed in a doorway and a fan draws in or expels air to pressurize or depressurize the home, typically to 50 Pa, with respect to outdoors. The volumetric flow rate can be obtained from the fan size and speed and the fan maintains this pressure difference across the entire envelope. The outputs of a blower door test include the overall coefficient between ΔP and volumetric flow, represented by K_{tot}, and the overall nature of the leakage, represented by n. The volumetric flow rate, Q_{fan}, is:

$$Q_{fan} = K_{tot}(\Delta P)^n \quad (3)$$

At elevated pressures, the entire flow through the fan makes up leakage through the building envelope. By measuring flow at several pressures, the method can yield values of K_{tot} and n, but in common practice, flow at a single pressure difference is reported, usually 50 Pa. Differences also occur within the same house depending on if the home was pressurized or depressurized. Discrepancies of about 20% for pressurization are commonly attributed to unidirectional dampers and mechanical ventilation that are more likely to be forced open during home pressurization [6].

Natural Causes of Cross-Envelope Pressure Differences

Natural pressures across the exterior, or envelope, of a home are dominated by two weather condition related forces: temperature-based pressures (stack effect) and wind impingement (wind effect). Fluctuations in indoor and outdoor temperatures and in outdoor wind speed mean that these pressures shift on a diurnal and seasonal basis, and thus the rate of natural infiltration changes as well.

Stack pressure is due to density differences between indoor and outdoor air; [7] therefore the magnitude of this pressure is largest when the indoor-outdoor temperature difference is greatest. The overall stack pressure P_s, or the maximum possible difference that may appear across the building envelope, is

$$P_{s,max} = (\rho_o - \rho_i)gh \tag{4}$$

where ρ_o and ρ_i are the outdoor and indoor densities, respectively, g is gravity, and h is the height of the conditioned space in the building. As written, P_s is positive when outdoor temperature is lower, and density higher, compared with indoors.

Wind pressures are created by the flow of air around the building. Wind pressures can be related to the wind velocity, V_{ref}, at an on-site location. Measurement of wind speed at or above the home height and without obstructions would result in the dynamic wind pressure:

$$P_w = \frac{1}{2}\rho V_{ref}^{\ 2} \tag{5}$$

Pressures across the envelope induced by wind depend on the orientation of the home with respect to wind direction, and shape of the structure and vary greatly between each face of the building. They also depend on vertical position z because wind speed tends to decrease with height and on the orientation of the average wind direction with respect to the building (θ). These dependences are indicated in the equation below:

$$P_w(\theta, z) = C_p(\theta, z)\left(\frac{1}{2}\rho V_{ref}^{\ 2}\right) \tag{6}$$

where $C_p(\theta, z)$ is a pressure coefficient. For free-standing buildings measured in wind tunnels, the value of C_p is maximum when the wind direction is perpendicular to the surface ($\theta = 0$), to decreases to zero until about $\theta = 60°$, and becomes negative at greater values of θ; that is, the effect of the flow field is to depressurize three faces of the building [8][9]. The greatest difference between the two faces is expected to occur between the windward and leeward faces.

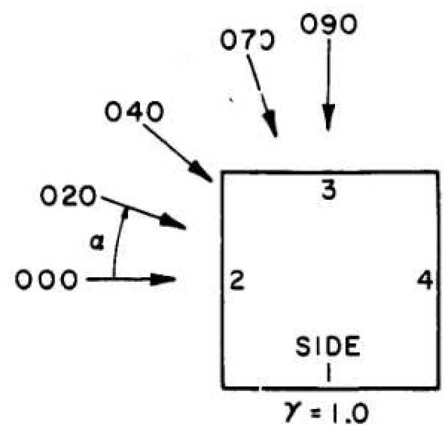

Figure 1. Example diagram of wind direction with relation to the faces of a building

Dependences on horizontal position, caused by the irregular shape of the flow field around the building, exist but are not shown in Equation (4) [10]. The flow field and hence the coefficients may be altered if other buildings or obstacles are near the structure of interest, and those values also vary with roof pitch [11]. The turbulent nature of wind also affects the measurement of coefficients in Equation (4), which decrease by about a factor of two when wind speed and pressure are averaged over periods of about 5 s, compared to averaging over 0.1 s [11].

The relationship between pressurizing effects and indoor air quality is outlined in Figure 2. The discussion above has covered the drivers of natural pressures across the building envelope (Fig. 2a) and maximum pressures that might be induced by these drivers (Fig. 2b). In the absence of mechanical ventilation, these natural driving forces dominate air flow and in turn the quality of air experienced by occupants (Fig. 2e). Determining how these pressures affect infiltration and exfiltration is the subject of the next sub-section.

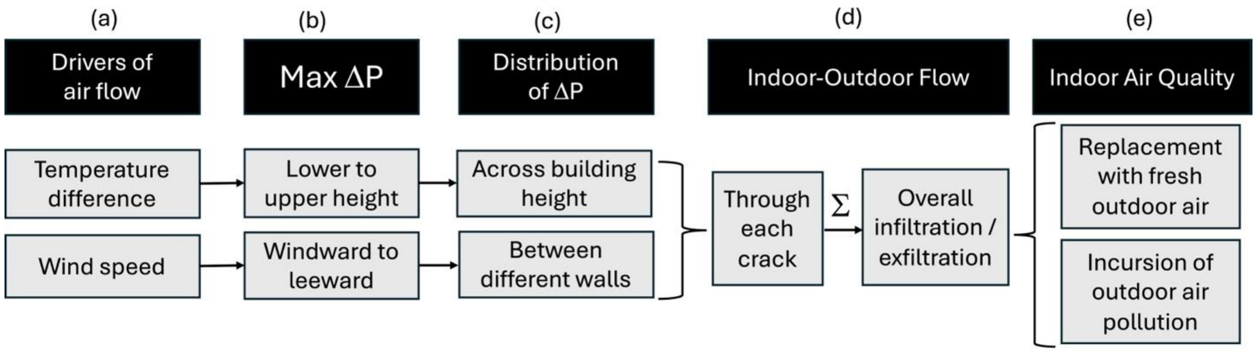

Figure 2. Relationship between environmental conditions, physical phenomena that drive indoor-outdoor exchange, and indoor air quality.

Estimates of Air Exchange Rates

The blower door test yields total building leakage and an average exponent, and Equation (1) would provide total flow if the pressure differential across the envelope was uniform. Infiltration prediction models such as the Lawrence Berkeley National Laboratory model (LBL) [12] and Alberta Infiltration Model (AIM-2) [13] estimate the magnitude of naturally driven infiltration (Fig. 2d) by estimating (a) how pressure differences are distributed across the building envelope (Fig. 2c); (b) the amount of leakage collocated with those pressures; and (c) the magnitude of airflow caused by those pressures. A key concept in these calculations is that infiltration, driven by positive pressure differences from outdoors to indoors, must balance exfiltration, driven by negative pressure differences from outdoors to indoors. Thus, the differential pressure is zero at some points on the building envelope, known as the "neutral point" or, for stack effect, the "neutral level." Of course, the exact position of each crack is not known, so infiltration models make assumptions about the fraction of leakage in the walls, ceiling, and floor, and assume the assigned leakage is uniformly distributed throughout those surfaces.

The LBL model by Sherman and Grimsrud assumes an exponent n of 0.5, so that for each crack, according to the Bernoulli equation:

$$Q_j = A_j\sqrt{\frac{2\Delta P_j}{\rho}} \tag{7}$$

The LBL estimate of infiltration flow induced by stack and wind, respectively, are:

$$Q_{stack} = f_s A_0\sqrt{\frac{P_{stack}}{\rho_0}} = f_s A_0\sqrt{gH\frac{\Delta T}{T}} \tag{8}$$

$$Q_{wind} = f_w A_0\sqrt{\frac{P_{wind}}{\rho_0}} = f_w A_0 v \tag{9}$$

where A_0 is the total leakage area and f_w and f_s are dimensionless parameters incorporating pressure and leakage distributions over the envelope. The model gives further guidance for inferring wind speed, v , from an offsite weather station measurement by correcting for height and shielding effects.

While similar in fundamental structure to the LBL model, the AIM-2 model has a few basic differences. It assumes non-zero pressure coefficients at the ceiling and floor; it calculates flow using the exponent n obtained from blower-door tests instead of the Bernoulli equation; and it includes leakage from furnace flues.

The LBL and AIM-2 models have substantially influenced both the theoretical understanding of infiltration dynamics and ventilation standards such as ASHRAE 62.2. Studies that can confirm the models' infiltration estimates are reviewed below.

Software-based models such as CONTAM simulate airflow paths, then use mass balance analysis between all building zones and outdoors to calculate building infiltration rates [14]. This model can account for complex building geometries, allowing simulations and evaluations of different residential designs. Although CONTAM is a powerful tool that can account for interzonal flows as well as the effects of HVAC systems, its assumptions about naturally driven infiltration also depend on measured leakage and theoretical pressure distributions described above. This model also requires knowledge of the location of leakage and the neutral point.

Measured Air Exchange Rates

Tracer gas measurements

One of the most common methods for estimating air exchange involves tracer gases. Tracer gas methods measure air infiltration and exfiltration by injecting a nonreactive gas into the home and monitoring the concentration. Variations of this method include constant injection, constant concentration, and single injection with concentration decay. The single injection method is most common due to the low financial and temporal expense of the approach. This method is considered the closest approximation to the true air exchange rate and therefore often used as a validation method for other airflow estimations. These methods are most accurate in well-mixed spaces and applicable in both occupied and unoccupied settings. The limitations of this technique include the necessity for specialized equipment, and varying expenses depending on the tracer gas that is used. Because of the assumption that the home operates as a single zone, the uncertainties surrounding the well-mixed condition and interzonal airflows can significantly affect confidence in estimates.

The concentration-decay method produces a single air exchange rate, which does not account for the dynamic nature of residential environments. Unless the method is repeated, it limits generalization to other times or seasons Bekö et al. conducted active and passive tracer gas experiments, measuring air exchange rates in homes across four seasons noting large variations in air exchange rates with respect to diurnal, seasonal changes, and the type of tracer gas utilized [15]. Wallace et al. conducted a year-long SF_6 tracer decay study in an experimental home to investigate how temperature, wind velocity, exhaust fans, and window-opening affected air change rates. The time series of air exchange determined from a series of tracer decay measurements was compared with temperature difference and wind speed, but not with modeled air exchange. The he largest influence on ACH was opened windows and the least was wind impingement [16].

Tracer gas comparison with measured leakage rates

One measure commonly communicated from blower door tests is ACH50 (Air Changes per Hour at 50 Pa). Although this value is simple to measure, a home is almost never at this high of a pressure differential. For context, a 50 Pa pressure is roughly equivalent to the pressure generated by a 20-mph wind blowing on the building from all directions, while pressure differences are typically -7.8 Pa and -5 Pa in mechanically ventilated and naturally ventilated buildings, respectively [17]. Efforts have been made to interpolate this 50 Pa condition to more realistic operating pressure differences. Persily estimated that the approximate air infiltration rate tends to be one-twentieth of the ACH50 value [18]. Sherman states that "although this expression ignores many details of the infiltration process, it appears to give qualitatively reasonable results for annual ensemble averages [19]." Pasos et al. compared blower door tests and CO_2 tracer decay tests in 21 homes in the UK. The study found that the divide-by-20 rule overestimates infiltration rates, suggesting a value closer to 37 is more accurate [20]. Because of the dynamic nature of infiltration, the divide-by-20 rule would not be expected to match point measurements of infiltration.

Time-resolved air exchange rates

Indoor and outdoor pollutant concentrations vary on the order of minutes, meaning that estimation of indoor-outdoor exchange for ventilation response would require prediction on this timescale. As Ng. et al states, "The dynamics are often simplified in ventilation standards and ventilation control strategies. For example, a single infiltration rate is often used, even though it may not be appropriate when determining whether the total outdoor air ventilation rate complies with a standard or local code requirement throughout the year" [21]. This author attempted to utilize real-time airflow estimates for residential ventilation control, to optimize the balance of energy use and air quality. However, there have been few measurements confirming infiltration model predictions on the order of minutes.

A common practice of weather based infiltration models is measurement of weather conditions away from the site, usually at airports, then correcting these values to determine wind speed at the site. This extrapolation is done with height corrections and multipliers that involve choosing shielding and terrain classes at the measurement site and the building site. However, the assignment of shielding and terrain correction values are "highly arbitrary" [22]. With the increased accessibility to onsite measurement tools there is new potential for more precise correlation between site weather conditions and infiltration.

Objective of Study

This study examines an intermediate step required to accurately predict time-resolved infiltration: pressures across the building envelope. If pressures cannot be well predicted from the driving forces of temperature difference and wind speed, neither can infiltration. The evaluation of predictability uses site-specific weather conditions to avoid errors in extrapolation from distant locations. This approach explores logistical advantages to pressure measurement in addition to testing the theory underlying infiltration predictions. If pressure measurements indicate when flow occurs through the building envelope, there is the potential for integration with HVAC systems to serve not only as thermal comfort systems, but also home pressurization systems intended for limiting exposure to poor air quality.

METHODS

Weather, home characteristics, and pressure measurements were collected in eight single-family residential buildings in the greater Fort Collins, Colorado area. These homes ranged in size from 1,358 to 3,640 ft^2 and are not representative of all Colorado or United States single-family residences. The observation period varied; five homes were observed for roughly six weeks, two homes were observed for nearly 12 weeks and one home was under observation for about a year. The length of time spent in the home was determined to be long enough to illustrate typical seasonal weather conditions and the envelope pressure response to them. While the longest observation period possible was ideal, the length was constrained to limit occupant disruption. Data was collected at a time resolution of minutes as this is the time scale in which the pressures that drive infiltration, and concentration of indoor and outdoor pollutants change.

Table 1: The duration of observation and home characteristics of all sites.

Site:	Duration:	Size (m^2):	Stack Height (m):	Home Type:	Foundation:
101	48 weeks	155	8.2	Townhouse (2 ext. walls)	Slab
231	7 Weeks	157	3.2	Split Level	½ Slab, ½ Crawl Space
241	6 Weeks	300	4.9	Detached Two-story	Basement
235	5 Weeks	163	4.7	Townhouse	Basement
234	11 Weeks	126	4.8	Townhouse (3 ext. walls)	Basement
227	12 Weeks	210	4.5	Split Level (3 ext. walls)	Slab
233	7 Weeks	338	4.6	Detached Two-story	Basement
229	7 Weeks	242	5.0	Split Level	½ Slab, ½ Basement

Description of home measurements

Time-resolved measurements

Table 2: The instruments placed in sites along with corresponding variables, and time resolution.

Instrument(s)	Variable	Method of Measurement	Time Resolution
Onset HOBO	Indoor Temperature RH	Thermistor	5 Minutes
AWAIR Omni	Indoor Temperature RH	Thermistor	5 Minutes
WeatherFlow Tempest	Outdoor Temperature RH	Thermometer	1 Minute
	Wind Speed Wind Direction	Ultrasonic Anemometer	
	Absolute Pressure	Barometer	
The Energy Conservatory (TEC) Dg1000	Indoor-Outdoor Differential Pressure	Diaphragm Manometer	5 Seconds

A WeatherFlow Tempest weather station was used to record outdoor weather conditions. The purpose of wind speed measurements was to determine whether on-site measurements could be useful in predicting pressures. In research on wind pressure coefficients, wind is often measured at the roofline height, and obstructions are nonexistent or placed in precise configurations. This placement was not possible in real homes and would not be reproducible in other homes. In practice, the optimal siting achievable at a real home was within the same property boundary; away from shielding by buildings or trees; free from theft possibilities; and as highly elevated as possible without the use of stabilizing wires. These limitations meant that wind speed was often measured below the roofline and relatively close to the structure.

For indoor temperature and relative humidity measurements either Onset HOBO thermistors or AWAIR Omni devices were utilized. The Omni devices were also able to record concentrations of CO_2, VOCs, particulate matter, noise, and light, however these will not be discussed.

The Energy Conservatory (TEC) Dg1000 manometers were used to capture differential pressure measurements. The placement of the manometers followed a three-location design: two high and one low. The high manometers were ideally on the same level on opposite ends of the home and the low pressure tap placed at the lowest position above grade in line with one of the high manometers. The actual orientation was influenced by the proximity to power outlets, layout of home walls and ceilings, and potential disruptions to home occupants. The taps were preferably placed on faces of the home that were not adjacent to other homes to limit shielding. The process of crossing the building envelope was done using one of two methods: a metal tap passed through a ⅛" hole drilled in the wall, or a metal tap passed through a window or door, subsequently sealed with tape. These prescriptions were ideal for stack and wind effect analysis, as described in the Data Analysis section, but could not be achieved in all homes.

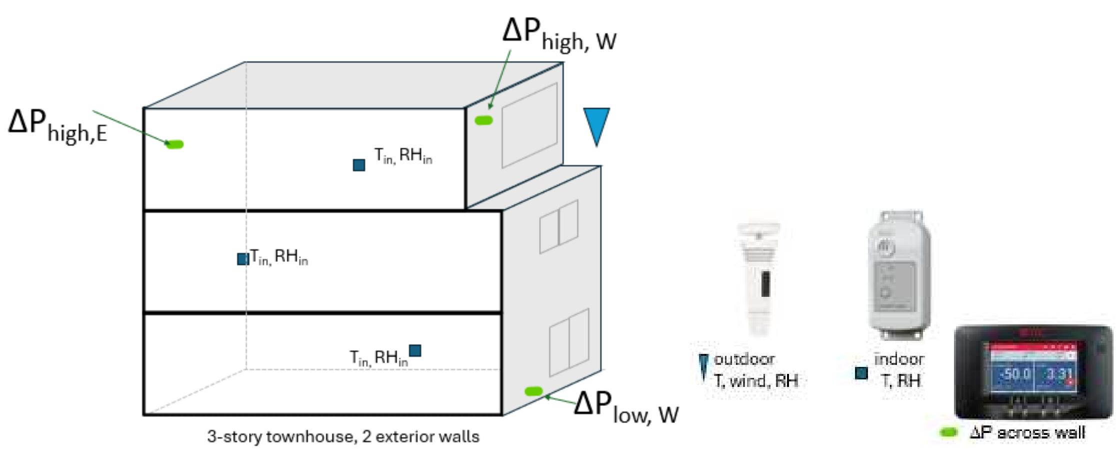

Figure 3: Example view of site faces with placement of weather station, thermistors and manometers

As the layout and inhabitant behavior was variable across homes, an important distinction was the characterization of the basement space. For most sites, the basement was considered an uninhabited buffer space as even if it was fully finished, it was mostly below grade and did not contribute to stack height. There were exceptions for homes that were split level, in which there was an inhabitable space partially below grade.

One-time measurements

At each site, a single fan, multi-point depressurization blower-door test was conducted. The household was depressurized at five Pa increments between 50 and 15 Pa and the volumetric flow value (Q_f) for each pressure was recorded.

Forms of mechanical ventilation typically used by site occupants were identified. All forms of ventilation were turned off and then each fan source was run independently for five-minute intervals to determine a pressurization signature for each source. A period of three to five minutes was taken between each test.

A LIDAR scan was conducted for all internal spaces of each home, which provided the internal volume and area of the occupiable spaces.

<u>*Data Analysis*</u>

Measured Stack Pressures

Figure 4 illustrates both the theoretical concept of stack pressure across the envelope and the strategy for observing it. Under heating conditions, outdoor air is colder and denser than indoor air, and pressure falls off more quickly with height than it does in indoor air.

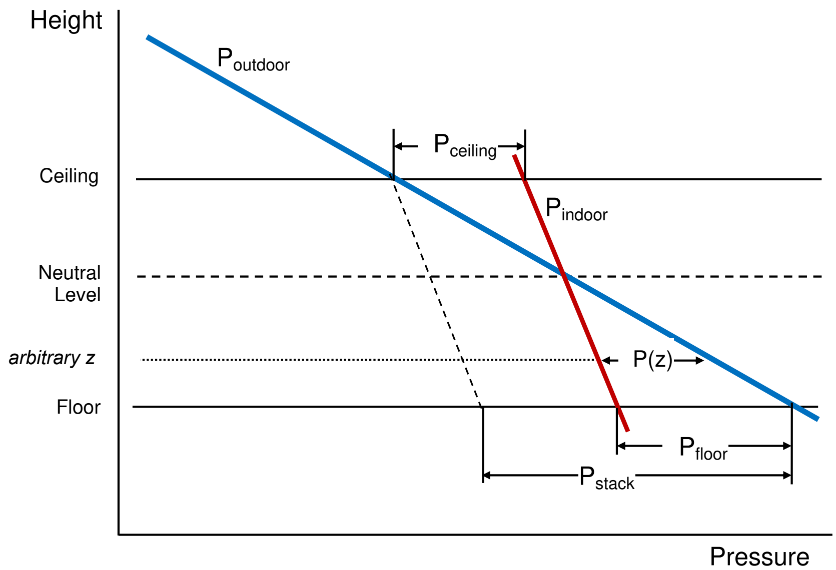

Figure 4: Diagram of pressure gradients inside and outside and their relation to stack pressure and neutral level. Heating conditions (indoor air warmer than outdoor air) are shown. Pressure gradients are exaggerated for illustration.

Under heating conditions, the pressure indoors is greater than outdoors at the ceiling, so the pressure differential $\Delta P_{high} = P_{inside} - P_{outside}$ is positive and results in exfiltration. Conversely, at the floor the pressure is higher outdoors and therefore the pressure differential $\Delta P_{low} = P_{inside} - P_{outside}$ is negative resulting in infiltration. The difference $\Delta P_{high} - \Delta P_{low}$ is the maximum amount of pressure difference (refer to Figure 1b). The stack pressure can be observed as the difference of cross-envelope delta-pressure (ΔP) measurements at the roofline and ground level of the home. Although no single point on the envelope experiences this total difference, it quantifies the maximum effect of the stack phenomenon.

Each ΔP measurement may be affected differently when wind is contributing to cross-envelope pressure. To reduce this effect, we placed the taps on the same face of the home. However, wind pressures at the upper and lower extremities of the home could be affected differently by wind speed and direction due to shielding, friction, and swirling. For that reason, we eventually examined stack effect only during low-wind conditions.

Predicted Stack Pressures

The predicted stack pressure was calculated with a slight modification to Equation 4. For the maximum stack pressure, the stack height is the height of the conditioned space. In practice, we measured slightly below the ceiling and slightly above the floor, so the predicted stack height for comparison used the distance between the high and low manometer taps:

$$P_{stack,obs} = (\rho_{out} - \rho_{in})gh_{high-low} \tag{11}$$

Temperature and relative humidity measurements for each level of the home were used to calculate the air density and using the Ideal Gas law. A sum of the level-based stack pressures provided the total stack pressure prediction.

Heating and cooling conditions were isolated to characterize seasonal variability. Heating conditions entailed any periods in which the indoor temperature was greater than outdoor temperature, with cooling conditions being all other observations.

Wind Cutoff

As the ΔP_{high} - ΔP_{low} proxy for stack pressure was most accurate when the impingement of wind was limited, a wind speed cutoff was used to remove periods of high wind effect for the stack analysis. While sites experienced differing magnitudes of wind speeds, 0.25 m/s was determined to be the threshold below which the effect of wind impingement was minimized.

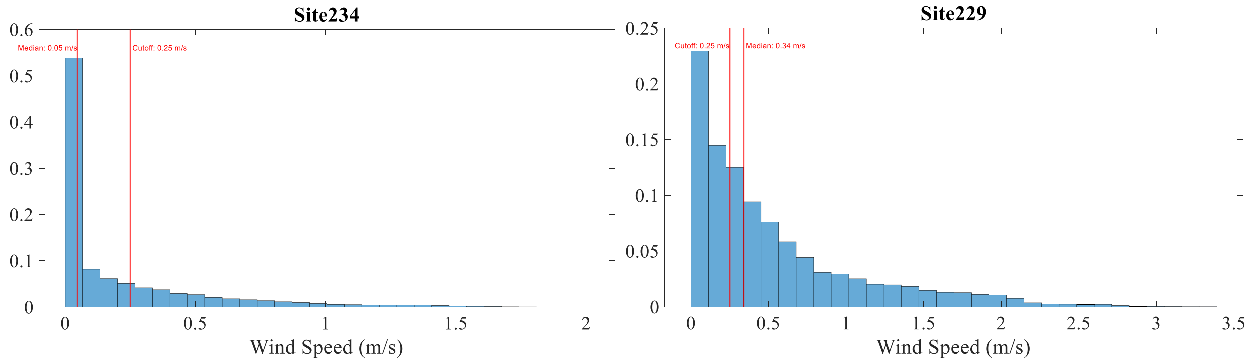

Figure 5: Distribution of wind speed in relation to default wind speed cutoff in sites: a) 234, and b) 229.

Weather station output for wind speed and direction were compared to three other stations in the Fort Collins and Loveland area, including the Northern Colorado Regional Airport, to determine well the site weather conditions represented the values experienced by the home.

Measured Wind Pressure

The observed wind effect was represented by the difference between the two pressure differences at the highest point of the home. Whenever possible, these two taps were placed at the same vertical level. Although the stack effect has an influence on all pressures, differencing two ΔP measurements at the same level removes this influence. The windward or upwind tap, which I will refer to as the tap or face of interest, was chosen based on the relationship between face direction, predominant wind direction, and weather station placement. The opposing or downwind tap pressures were then subtracted from the windward pressure providing a representation of the pressure effect due solely to the presence of wind. The pressure across the upwind (*upw*) and downwind (*dnw*) walls at height *z*, expressed in terms of their coefficients, is:

$$\Delta P_{upw,high}(z) = \Delta P_{stack}(z) + C_p(\theta_{upw}, z)P_{wind,dyn} \tag{12a}$$

$$\Delta P_{dnw,high}(z) = \Delta P_{stack}(z) + C_p(\theta_{dnw}, z)P_{wind,dyn} \tag{12b}$$

and the difference of the two ΔP values is an observed wind effect:

$$P_{wind}(z) = \left[C_p\left(\theta_{upw}, z\right) - C_p(\theta_{dnw}, z)\right]P_{wind,dyn} \tag{12c}$$

Interpretation of Wind Pressure Coefficients

A simple dynamic wind pressure was calculated using the measured wind speed:

$$P_{wind,dyn} = \frac{1}{2}\rho V^2 \tag{13}$$

The expected wind pressure would be a direction-dependent coefficient multiplied by $P_{wind,dyn}$. Because the weather stations were located below the roofline, with reduced wind speeds, coefficients might be expected to be greater than for dynamic pressures based on roofline wind speed. Table 3 shows the difference between the height of the weather station and the highest measured pressure tap.

Table 3: The height of the Tempest weather station at each site and its relation to the highest pressure measurement and home structure.

Site	Height (m)	Distance below Tap (m)	Relative Location
101	7.2	-1.2 / 0.5*	4 m West of home
231	2.4	0.8	5 m East of home
241	3.0	1.9	4 m South of home
235	2.1	2.6	0.6 m North of garage
234	2.7	2.1	3 m East of home
227	2.7	1.8	3 m West of home
233	2.7	1.9	6 m South of home
229	2.7	1.6	6 m South of home

*For the first four months of measurement, the weather station was above tap before the tap was moved to a higher position

In addition to comparison of the dynamic wind pressure and the observed wind influence, effective coefficients were also extracted from individual tap measurements. Assuming the differential pressure is a summation of stack and wind effect, a linear relationship can be constructed such that:

$$\Delta P(z) = \alpha(z)P_{stack} + C_p(\theta, z)P_{wind,dyn} \tag{14}$$

where α accounts for the vertical distribution of stack pressure. A lower wind speed cutoff is useful for this analysis as the contribution of wind pressure is minimal when wind speed is below a certain threshold. The uniform wind speed cutoff for all sites was 0.5 m/s.

The actual wind pressure experienced by the building face is also known to have dependency on wind direction [8]. Data points were divided into 30° bins by wind direction and then coefficients were determined by linear regression.

Offsite Wind Correction

As LBL and AIM-2 both use airport wind measurements for quantification of wind pressure, the offsite wind speed and shielding correction derived in the LBL model were calculated for wind measurements taken at the Northern Colorado Regional Airport. The equation for this conversion is as follows:

$$v_{corrected} = v_{airport}\left(\frac{\alpha\left(\frac{H_{ceiling}}{10}\right)^{\gamma}}{\alpha\prime\left(\frac{H_{airport}}{10}\right)^{\gamma\prime}}\right) \tag{15}$$

Sites were classified as terrain Class III and the airport was classified as terrain Class II with α and γ constants obtained from Sherman and Grimsrud (1980) table A1. The height of the airport, $H_{airport,}$ anemometer was assumed to be ten meters.

Mechanical Ventilation

Mechanical ventilation is a contributor to pressure and airflow, but our use of the difference of pressure differentials for this analysis minimizes its influence. However, as mechanical ventilation typically affects the interior pressure of the home uniformly, its influence cancels out in the difference between the cross-envelope ΔPs.

Minimal influence of mechanical ventilation

This work examines naturally driven pressures, and it is desirable to examine those pressures in the absence of mechanically driven ventilation. The influence of mechanical ventilation appears within the pressure data as step-function periodic pressurization and depressurization that was regular on the order of minutes to hours, as shown in Figure 6a for Site 233. In this case, mechanical ventilation induces internal depressurization of around 1.5 Pa. However, ventilation affects all pressures similarly. Once the two cross-envelope ΔPs are subtracted (Figure 6b), fluctuations in the stack pressure are nearly cancelled out, with remaining small fluctuations of about 0.25 Pa.

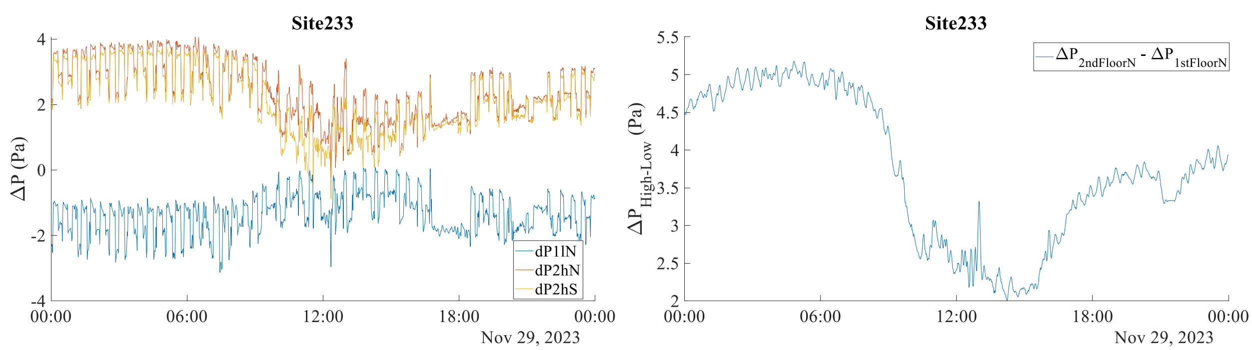

Figure 6: a) The three differential pressure signals in response to mechanical ventilation in site 233; b) and the resultant stack equivalent difference between two of the pressure signals.

Stack Effect

Analysis of stack pressure included the comparison of predicted and observed values, with particular interest in conditions that have a significant impact on their agreement. Two examples of good prediction-observation agreement are shown in Figure 7. Stack predictions agree with measurements rather well on these 1-minute time scales, even matching some of the short excursions 1-2 hours in length.

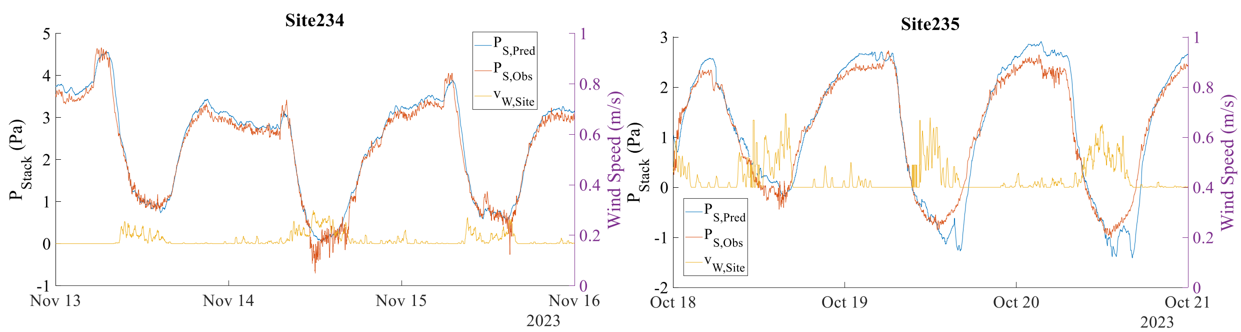

Figure 7: Predicted and observed stack pressures at sites 234 and 235 under heating and low wind conditions.

During periods of elevated wind speed, the stack pressure observation – the difference between high and low pressures on the same wall - was no longer smoothly varying and also deviated from predicted stack pressure (Figure 8). This observation indicates that two taps on the same wall did not experience the same wind pressure,so the subtraction of pressure differences did not yield a stack pressure alone.

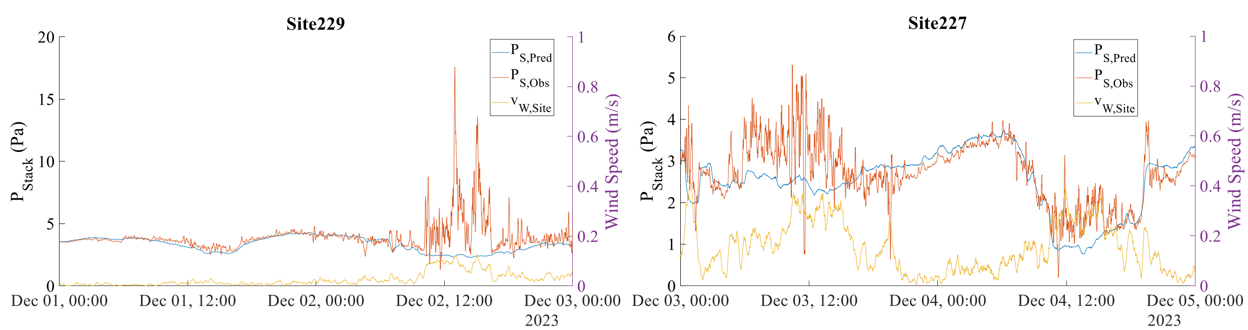

Figure 8: Predicted and observed stack pressures at site 229 and 227 sites during periods of elevated wind speed

Under cooling conditions, when the temperature indoors is cooler than outdoors, stack predictions also deviate from the theoretically established pressure predictions. Neither wind speed influence nor floor-to-floor stratification explain this discrepancy. These deviations did not appear in all sites because only two sites had more than 25% of observations in the cooling regime. Further data collection in cooling conditions is needed to better understand these dynamics.

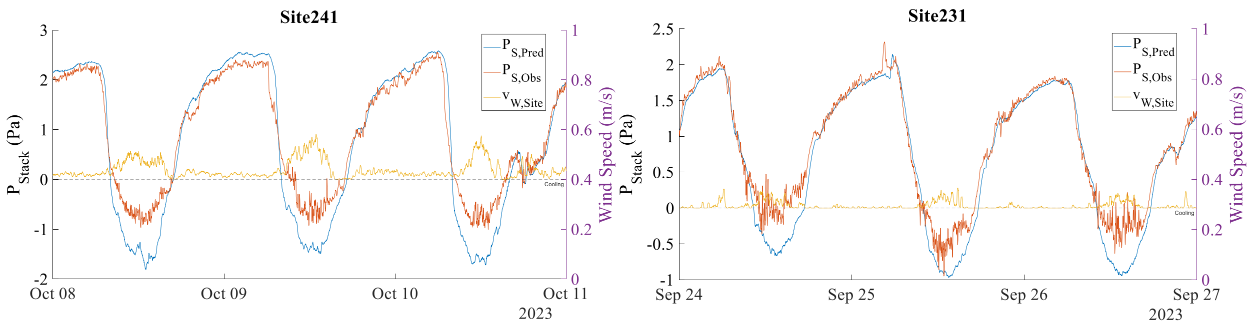

Figure 9: Examples of divergence between predicted and observed stack pressures in cooling conditions.

Mean absolute errors (MAE) of predicted stack pressures are summarized in Table 4. As wind speed and cooling conditions were shown to influence stack pressure prediction, MAE values were calculated for filtered data in addition to all data. The mean absolute error overall was greater for sites 101, 233 and 229, which had a greater fraction of high wind speed and cooling conditions. For low-wind conditions, all sites had very similar MAE values, less than or equal to 0.35 Pa across varying months. These findings demonstrate a strong relationship between theoretically predicted and observed stack pressures. Most of the errors between stack pressure predictions and observed pressure measurements occur during periods of high wind. For instance, site 231 had the lowest overall MAE of 0.21 Pa, but 90% of its observations were in the low wind regime. It appears to have a lower MAE than sites 233 and 229, for which the low wind regime only accounted for about 50% of observations; when high-wind conditions are removed, the MAE values are similar.

Table 4: Length of observation, 10th and 90th percentile of stack pressures, and Mean Absolute Error under three conditions, for one-minute data.

			MAE[a] Observed-Predicted (Pa)		
Site	Obs Dates	10 - 90% Stack P (Pa)	All	Low Wind (% obs)	Low Wind & Heating[b] (% obs)
101	10/22 – 11/23	0.3 - 6.6	0.81	0.31 (32)	0.25 (28)
231	8/23 – 10/23	-0.2 - 1.8	0.21	0.17 (90)	0.11 (67)
241	9/23 – 10/23	-0.4 - 2.4	0.30	0.20 (62)	0.16 (53)
235	9/23 – 10/23	-0.4 - 2.4	0.26	0.27 (74)	0.27 (66)
234	10/23 – 1/24	1.2 - 4.5	0.33	0.23 (71)	0.23 (71)
227	10/23 – 1/24	1.5 - 4.8	0.33	0.22 (32)	0.22 (32)
233	11/23 – 1/24	2.0 - 5.0	0.56	0.35 (63)	0.35 (63)
229	11/23 – 1/24	1.9 - 5.2	0.99	0.16 (41)	0.16 (41)

[a] MAE: Mean absolute error. [b] The T_{in} of lowest living space is greater than or equal to T_{out}.

During heating conditions, predictions were more accurate particularly for the two sites that experienced periods of cooling conditions. At Site 231, the MAE was 0.17 Pa during low wind conditions, decreasing to 0.11 Pa under low wind and heating conditions: a 47.6% improvement over low wind conditions alone. Similarly, Site 241 had an MAE of 0.20 Pa under low wind conditions and decreased to 0.16 Pa under low wind and heating conditions: a 20% enhancement. To contextualize the MAE values, the power relationship between differential pressure and flow developed in Equation 4 can be used. Given a desired error in air flow (Q_{error}/Q_{true}) of 10% or less, and the default exponent value "n" is roughly 0.65, the allowable percent error for predicted pressures is around 15%. Infiltration is greatest when pressure is greatest so by comparing the MAE values to the 90th percentile stack pressures, the percent error at the most substantial pressures can be observed. Site 229 was the only site in which the MAE was outside of the desired percent error and once high wind events were removed, this site also fell within the desired error ranges.

Table 5: Coefficient of Determination (R^2) for the stack effect prediction for all sites under three key conditions.

	R^2		
Site	All	Low Wind	Low Wind & Heating
101	0.556	0.947	0.929
231	0.853	0.932	0.903
241	0.937	0.944	0.916
235	0.949	0.939	0.900
234	0.818	0.908	0.901
227	0.822	0.980	0.980
233	0.682	0.964	0.970
229	0.070	0.939	0.939

R^2 values were calculated for the same overall, low wind, and low wind plus heating conditions as MAE. For most sites, an average of 87.5% of the $\Delta P_{high} - \Delta P_{low}$ observed stack pressure variance could be explained by the theoretically derived stack pressure prediction across all observations. By isolating only predicted and observed pressure values that coincided with wind speeds below the site-specific cutoffs, the predicted stack pressure explained a vast majority of the remaining variance in the observed stack pressures. After removing high-wind observations, stack pressure predictions on average explained over 92% of the observed stack pressure variance. The site with the largest increase in variance explained was site 229. This indicates a large and consistent influence of wind on the observed stack measurement for this site especially.

In summary, stack pressure is well predicted under low wind and heating conditions, with MAE of 0.1-0.3 Pa across all sites; this is well within the 15% error that would produce air flow predictions with 10% error or less. This level of predictability for one-minute data is exceptional and unexpected. R^2 values indicated that the theoretical stack pressure predictions explained over 92% of the variance in observed pressures, particularly when high wind periods were excluded. While cooling conditions were only consistently seen in two sites, predictions during these periods were less accurate, with discrepancies not fully explained by wind effect or temperature stratification.

Wind Effect

Periods of episodic pressurization or depressurization could be attributed to windy periods, as indicated by spikes of wind speed at the site weather station. However, elevated pressure was often maintained even when the recorded wind speed was low or zero.

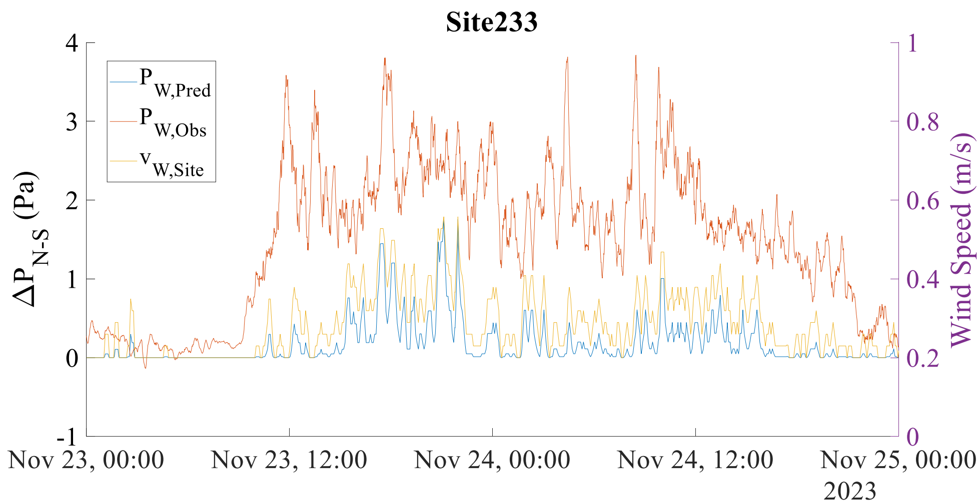

Figure 10: Predicted and observed wind pressures during a period of consistent wind at site 233

The magnitude of the dynamic wind pressure was lower than the observed wind pressures; that is, the predicted coefficient differential was much greater than one. This difference could have been due to the height difference between the weather station and the manometer taps (Table 3) or shielding from nearby obstructions as well as the actual wind pressure coefficient.

While wind speed did not correlate with wind pressure on a minute-to-minute basis, there may be a general relationship between predicted and observed wind pressure . In all cases, prevalence of wind speeds above the threshold of 0.5 m/s was a strong indicator of observed pressurization. This correlation between the speed of wind and the corresponding observed pressure is shown in Figure 11. Sites 227 and 229 showed the most consistent linear relationship, however the slopes of the relationships were dissimilar in these sites, as shown in Table 6.

In Site 227, much of the observed wind pressure is explainable by with the predicted wind pressure (R^2 = 0.571). A similar strong relationship is also apparent in Site 229 (R^2 = 0.532), although data at this site show a secondary, negative slope. This duality shows the influence of wind direction, which is explored in the next section.

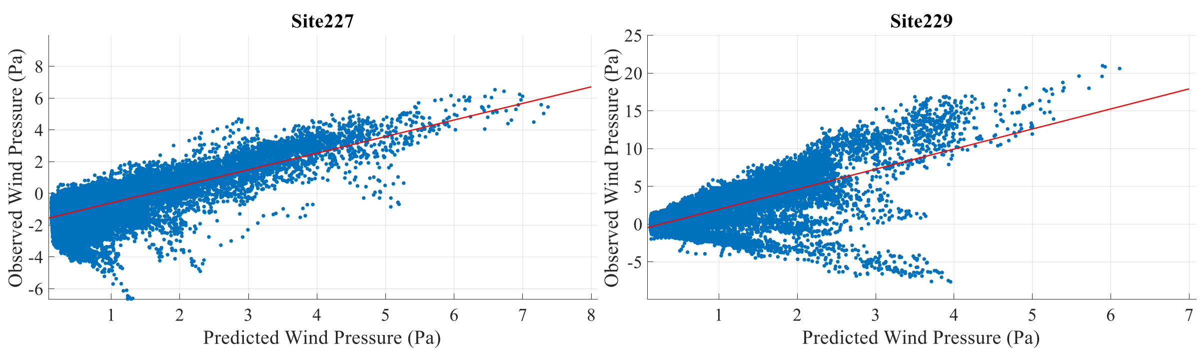

Figure 11: Observed correlation between wind speeds and pressurization in site 227 and 229

Most other sites displayed variable wind pressure responses to wind speed. These values are summarized in Table 6. Site 234 is excluded from the table because the pressure measurements were not placed on opposite faces. Site 241 (Figure 11) had one of the lowest R^2 values, indicating a negligible linear correlation; the figure also shows that wind speeds remained low at this site.

Table 6: Evaluation of linear relationship between wind speed and pressure with R^2 values.

Site	Slope	R^2
101	1.387	0.397
231	2.068	0.097
241	0.544	0.007
235	0.413	0.157
227	1.044	0.571
233	0.183	0.153
229	2.657	0.532

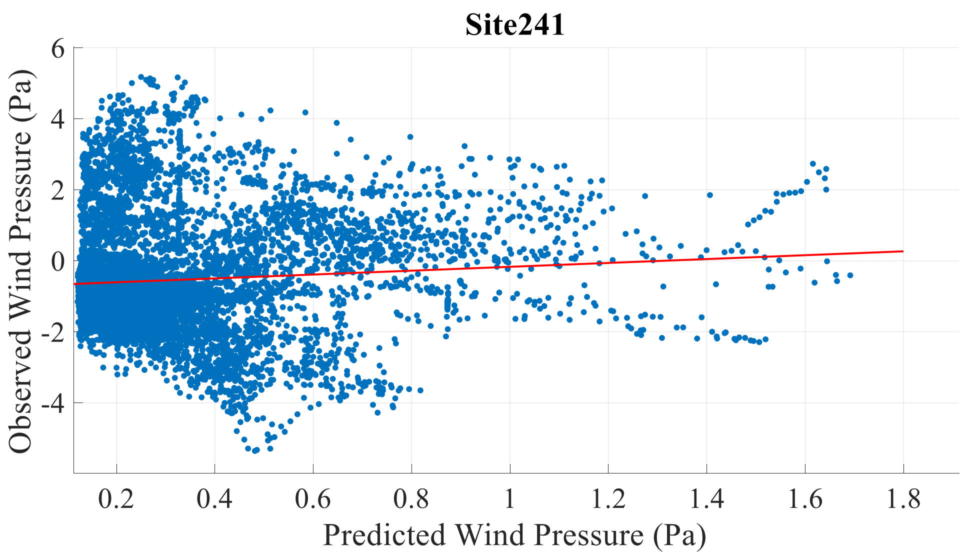

Figure 12: Lack of correlation between wind speeds and pressurization in site 241

To examine the directionality of wind influence, regressions were done on individual ΔP data according to Equation 14, separately within each bin of 30 degree wind direction. An example of the effective coefficients for one site is shown in Table 7.

Table 7: Effective coefficients for wind pressure on all three cross-envelope taps at site 229 and their changes with wind direction. Asterisk indicates an R^2 value greater than 0.5.

	Effective Coefficient		
Wind Direction (°)	$\Delta P_{GroundFloorSouthwest}$	$\Delta P_{2ndFloorSouthwest}$	$\Delta P_{2ndFloorNortheast}$
15	0.220*	1.602*	0.101
45	0.248	1.266	0.413
75	0.324	2.334	0.908
105	0.706	4.791*	2.145
135	0.931*	6.015*	2.601*
165	0.826	5.667*	2.644*
195	0.741	5.126	2.044
225	0.598	3.640	1.136
255	0.730	2.857	1.131
285	0.597	3.384	1.126
315	0.447	2.998	0.375
345	0.412	2.183	-0.465

The coefficients shown in Table 6 show two unanticipated characteristics that appear in this site and others. The first finding, for sites 101, 231, and 229 showed very little discernable change in coefficient when the direction of incident wind changes. This outcome does not match findings observed in idealized flow fields, where pressurization is relatable to whether the wind is directly on, parallel to, or opposite of, the face. This finding suggests architectural features, local shielding, and wind patterns have substantial influence on the directional nature of wind pressures.

The second characteristic, unique to sites 234, 233, and 229, was the similarity in the sign and magnitude of coefficients between opposite-facing pressures for nearly all wind angles. Taps on opposing walls are expected to have opposite signs of response to wind.

In summary, elevated winds do have an influence on building pressurization, but the minute-to-minute prediction is not as reliable as that of the stack effect. Rather than following wind speed fluctuations directly, the pressure influence occurs over the entire period when elevated wind is present. General coefficients expressing wind dependence are dissimilar between sites, and accounting for wind directionality does not improve the predictability.

Airport Correction

Site wind speed and direction measurements showed significant and nonconstant deviation from those obtained from other local stations, including airport measurements that are typically used in LBL and AIM-2 estimates.

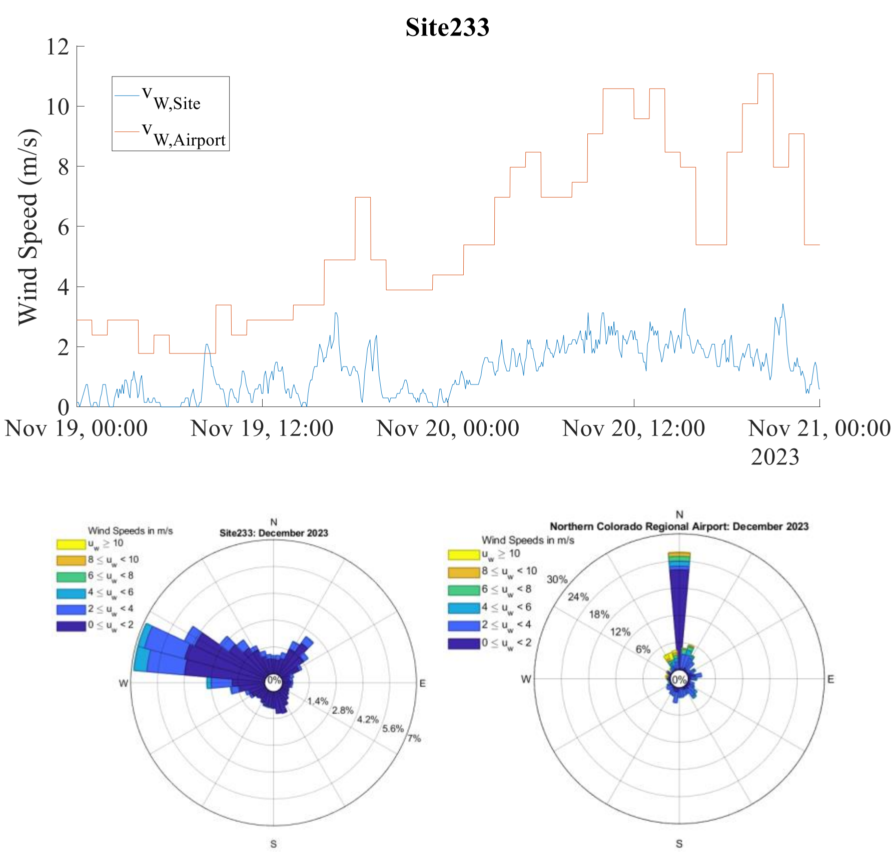

Figure 13: a) Deviation between airport and site 233 wind speeds b) Comparison between monthly averaged site wind speed and direction measurements at airport and site 233.

Peaks of wind speed at the Northern Colorado Regional airport weather station tended to be roughly five times larger than those reported at site 233, with this difference being consistent across other sites and times.

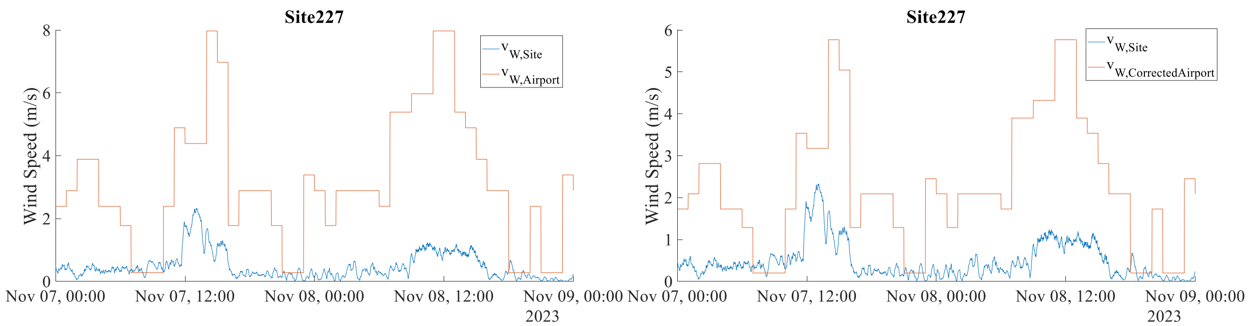

Figure 14: Comparison of airport and site wind speed a) before and b) after LBL correction

Figure 14 shows a comparison between the raw wind speeds before and after height and shielding correction developed in the LBL model. Although the correction factor does make the airport wind speed values more like the values recorded onsite, the corrected airport wind speeds still tended to be three or more times greater than the site speeds.

Individual point predictions and MAE values that mirror those calculated for stack pressure are complicated by the following conditions for wind pressure. First, the noisiness and instability of the observed wind pressure data makes accurate and reliable predictions difficult. Secondly, the effective coefficients did not explain wind directional pressurization, meaning that the sign and magnitude of the pressures were not conducive to prediction.

Without reliable wind pressure point predictions, and the temporally nonconcurrent nature of stack and wind effects, their combination is not suitable to an interpretable total pressure prediction. There also was no established proxy for the observed whole home pressure to compare to, as the observed pressures were measured as differentials between inside and outside. For these reasons the combination of the two effects was not attempted here and requires further study.

Sporadic pressurization or depressurization typically aligned with periods of elevated wind speed recorded by the site weather station. However, predicted wind pressures were often lower than observed values, likely due to height differences and shielding effects. The largest divergence between predicted and observed wind pressures occurred during high wind speed events. Sites 227 and 229 showed weak linear relationships between wind speed and observed pressure, while all other sites showed no correlations. Airport wind speed and direction measurements were not representative of those at the site, even after the use of height and shielding corrective equations. This indicated that these measurements are not conducive for use in predictive site pressures or behaviors.

Outlook

Stack pressure is predicted exceptionally well under low-wind and heating conditions, and indoor and outdoor temperature data can be used to obtain an accurate, time-resolved measurement of stack pressure. Additional observations are needed to understand why the stack prediction is not as accurate under cooling conditions.

Wind pressures are associated with elevated wind but are not predictable from theory. Estimating building-face pressures probably requires determining site-specific, face-specific coefficients; even then, observed pressures do not correlate directly with wind speed on a time resolution of minutes. Wind directionality does not explain variation, either. Furthermore, even if wind pressures were predictable, site wind speeds do not have a good relationship with airport wind data, so that estimation of wind pressures would require site wind measurements. Because the wind pressure could not be predicted accurately using site or airport measurements on a time resolution of minutes, wind's contribution to total home pressure could not be attributed accurately. There were periods in which wind was influential to and dominating of envelope pressurization indicating that its effects should not be discarded. Further study into wind's pressurization would explore the nature of local shielding.

CONCLUSION

This study examined the theoretical relationship between weather conditions and their effects on residential envelope pressures over observation periods that highlighted seasonal variability and timesteps that reflect the transient nature of air exchange and pollutant variance. The focus on minute-level time steps not only bridged theoretical gaps but also opens the door for better understanding and control of infiltration dynamics.

Key findings revealed that the influence of wind had a confounding influence on stack pressure prediction. When removing instances of wind higher than the wind speed cutoff, the average MAE of the predicted pressure was 0.24 Pa for all sites. As most sites had a trivial number of cooling events, the values obtained from removing these periods showed similar results to those found under solely low wind conditions.

The magnitude and direction of observed wind pressures could not be accurately predicted from site weather conditions due to their intermittent and sporadic influence on building face pressure. However, wind speed events above the threshold of 0.5 m/s were excellent indicators of pressurization and the general correlation between wind speed and observed wind pressurization were obtained.

The comparison of airport and site weather data found that there were significant differences in both wind speeds and directions. Even after the use of correction for shielding and height difference, there remained a large deviation between these values indicating that airport weather does not well represent the conditions recorded near the site.

This research underlines the influence of high-resolution data in accurately modeling residential infiltration dynamics. Future studies could expand upon this work by exploring the integration of predictive models with smart home technologies, thereby enhancing the ability to dynamically manage indoor air quality in response to both predicted and real-time environmental changes.

REFERENCES

[1] N. Klepeis *et al.*, "The National Human Activity Pattern Survey (NHAPS): A resource for assessing exposure to environmental pollutants," *Journal of exposure analysis and environmental epidemiology*, vol. 11, pp. 231–52, Mar. 2001, doi: 10.1038/sj.jea.7500165.
[2] A. Sfakianaki *et al.*, "Air tightness measurements of residential houses in Athens, Greece," *Building and Environment*, vol. 43, no. 4, pp. 398–405, Apr. 2008, doi: 10.1016/j.buildenv.2007.01.006.
[3] A. Persily, A. Musser, and S. J. Emmerich, "Modeled infiltration rate distributions for U.S. housing: Modeled infiltration rate distributions," *Indoor Air*, vol. 20, no. 6, pp. 473–485, Dec. 2010, doi: 10.1111/j.1600-0668.2010.00669.x.
[4] "ASHRAE - Standard 62.2." Accessed: Jul. 15, 2024. [Online]. Available: https://ashrae.iwrapper.com/ASHRAE_PREVIEW_ONLY_STANDARDS/STD_62.2_2022
[5] D. T. Grimsrud, H. H. Sherman, R. C. Diamond, P. E. Condon, and A. H. Rosenfeld, "Infiltration-Pressurization Correlations: Detailed Measurements on a California House." ASHRAE TRANSACTIONS, 1979.
[6] W. R. Chan, J. Joh, and M. H. Sherman, "Analysis of air leakage measurements of US houses," *Energy and Buildings*, vol. 66, pp. 616–625, Nov. 2013, doi: 10.1016/j.enbuild.2013.07.047.
[7] G. T. Tamura and Shaw, C Y, "Studies on exterior wall air tightness and air infiltration of tall buildings," *ASHRAE Trans.*, vol. 82, 1976.
[8] R. E. Akins, J. A. Peterka, and J. E. Cermak, "AVERAGED PRESSURE COEFFICIENTS FOR RECTANGULAR BUILDINGS," in *Wind Engineering*, Elsevier, 1980, pp. 369–380. doi: 10.1016/B978-1-4832-8367-8.50041-3.
[9] M. Grosso, "Wind pressure distribution around buildings: a parametrical model," *Energy and Buildings*, vol. 18, no. 2, pp. 101–131, Jan. 1992, doi: 10.1016/0378-7788(92)90041-E.
[10] D. Cóstola, B. Blocken, and J. L. M. Hensen, "Overview of pressure coefficient data in building energy simulation and airflow network programs," *Building and Environment*, vol. 44, no. 10, pp. 2027–2036, Oct. 2009, doi: 10.1016/j.buildenv.2009.02.006.
[11] Y. Uematsu and N. Isyumov, "Wind pressures acting on low-rise buildings," *Journal of Wind Engineering and Industrial Aerodynamics*, vol. 82, no. 1–3, pp. 1–25, Aug. 1999, doi: 10.1016/S0167-6105(99)00036-7.
[12] M. H. Sherman and D. T. Grimsrud, "INFILTRATION-PRESSURIZATION CORRELATION: SIMPLIFIED PHYSICAL MODELING," 1980.
[13] L. Walker, "THE ALBERTA AIR INFILTRATION MODEL," 1990.
[14] A. Persily, L. Ng, W. S. Dols, and S. Emmerich, "Techniques to Estimate Commercial Building Infiltration Rates," *40th AIVC*, 2019.
[15] G. Bekö *et al.*, "Diurnal and seasonal variation in air exchange rates and interzonal airflows measured by active and passive tracer gas in homes," *Building and Environment*, vol. 104, pp. 178–187, Aug. 2016, doi: 10.1016/j.buildenv.2016.05.016.
[16] L. A. Wallace, S. J. Emmerich, and C. Howard-Reed, "Continuous measurements of air change rates in an occupied house for 1 year: The effect of temperature, wind, fans, and windows," *J Expo Sci Environ Epidemiol*, vol. 12, no. 4, pp. 296–306, Jul. 2002, doi: 10.1038/sj.jea.7500229.

[17] V. Leivo, M. Kiviste, A. Aaltonen, M. Turunen, and U. Haverinen-Shaughnessy, "Air Pressure Difference between Indoor and Outdoor or Staircase in Multi-family Buildings with Exhaust Ventilation System in Finland," *Energy Procedia*, vol. 78, pp. 1218–1223, Nov. 2015, doi: 10.1016/j.egypro.2015.11.188.
[18] A. Persily, "Understanding Air Infiltration in Homes," Princeton University, 1982.
[19] M. H. Sherman, "Estimation of infiltration from leakage and climate indicators," *Energy and Buildings*, vol. 10, no. 1, pp. 81–86, Feb. 1987, doi: 10.1016/0378-7788(87)90008-9.
[20] A. V. Pasos, X. Zheng, L. Smith, and C. Wood, "Estimation of the infiltration rate of UK homes with the divide-by-20 rule and its comparison with site measurements," *Building and Environment*, vol. 185, p. 107275, Nov. 2020, doi: 10.1016/j.buildenv.2020.107275.
[21] L. C. Ng, S. Zimmerman, J. Good, B. Toll, S. J. Emmerich, and A. K. Persily, "Estimating real-time infiltration for use in residential ventilation control," *Indoor and Built Environment*, vol. 29, no. 4, pp. 508–526, Apr. 2020, doi: 10.1177/1420326X19870229.
[22] L. Palmiter and T. Bond, "Modeled and Measured Infiltration," 1991.